



## **Electric Field of a Homogeneous Charged Volumetric Hemisphere Over Its Symmetry Axes**

**Pablo Marón<sup>1</sup> & Ángel del Vigo<sup>2\*</sup>**

<sup>1</sup>Escuela Politécnica Superior, Universidad Antonio de Nebrija, Madrid (Spain)

<sup>2</sup>E.T.S.I. Topografía, Geodesia y Cartografía, Universidad Politécnica de Madrid, Madrid (Spain)

\*Corresponding author: [a.delvigo@upm.es](mailto:a.delvigo@upm.es)

**Abstract:** Analytical study of homogeneous charged volumetric hemisphere electric field along its symmetry axes is presented in this article. Solution was obtained by two different ways; on one hand, superposition of finite thickness disks with increasing radius, and, on the other hand, straightforward integration of finite volume elements in cylindrical coordinates. The same result is obtained in both cases. Additionally, a numerical solution based on the electric field created by a random distribution of discrete charges inside the hemisphere was calculated to check the analytical solution. Concordance between the analytical and numerical solutions was found. The interest of this theoretical result at electronics investigation field resides on its utility to determine the capacity of two opposite hemispheres capacitor system.

**Keywords:** Coulomb's law, electrostatics, hemispherical capacitor

## **Medan Listrik pada Hemisfer Volumetrik Bermuatan Homogen di Atas Sumbu Simetrinya**

**Abstract:** Studi analitis medan listrik hemisfer volumetrik bermuatan homogen sepanjang sumbu simetrinya disajikan dalam artikel ini. Solusi diperoleh dengan dua cara berbeda yaitu superposisi cakram ketebalan terbatas dengan radius yang meningkat, dan integrasi langsung elemen volume terbatas dalam koordinat silinder. Hasil yang sama diperoleh dalam kedua kasus. Selain itu, solusi numerik berdasarkan medan listrik yang dibuat oleh distribusi acak muatan diskrit di dalam hemisfer dihitung untuk memeriksa solusi analitis. Konkordansi antara solusi analitis dan numerik ditemukan. Minat hasil teoritis ini di bidang investigasi elektronika terletak pada kegunaannya untuk menentukan kapasitas sistem kapasitor dua hemisfer yang berlawanan.

**Kata kunci:** Electrostatics, hemisfer kapasitor, hukum Coulomb

### **INTRODUCTION**

Study of charged continue system electric field is a classical problem of electrostatics (Feynman *et al*, 1972). Symmetry of the body, charge uniformity and the place where electric field is calculated, determines the difficulty of the problem's solution (Griffiths, 2017). Classical books of Physics, Electricity and Electromagnetism (Eisberg & Lerner, 1988; Purcell, 1988; Jackson, 1998; Tipler & Mosca, 2010) gives solution of this problem by the integration of Coulomb's law, for cases where exists a high symmetry conditions such as homogeneous charged segments, rings or disks along its symmetry axes. Gauss law, which is a derivation of the Coulomb law (Jackson, 1998; Griffiths, 2017), is also used whenever conditions of high symmetry electric field flux exist along any closed gaussian surface.

Homogenous charged hemisphere electric field is not a complete symmetric vector field since spherical symmetry is broken when one half of the sphere vanishes. In a previous article (del Vigo & Renedo, 2016) electric field of a homogeneously charged hemispherical surface along its symmetric axes was obtained. This result that was validated by numerical integration, led to correct a previous solution published in the bibliography for this system (Burbano *et al*, 2004).

This paper presents the study of the electric field of a homogeneously charged solid hemisphere along its symmetry axis. The integration of the equations for this system is some more complicated (and longer) than the case of the hemispherical surface because it also contains charge interior.

The geometry of this system is not appropriate for the application of Gauss law with simplicity due to the lack of symmetry for the electric field flux as discussed in the bibliography (del Vigo & Villarino, 2020). On the other hand, analytical integration via Coulomb's law is possible, despite it can be long. In this way, a superposition of finite thickness disks of increasing radius solution is given in this article. Furthermore, a second analytical solution based on the direct integration of Coulomb's law for finite volume elements of charge  $dq$  is presented arising the same result. At the end of the article, numerical approximation to the solution based on electric field superposition of a randomly placed discrete set of charges inside the hemisphere is given. This numerical result corroborates the validity of the analytical solution obtained.

The interest of this solution, which was not found in the bibliography, as the previously mentioned for the hemispherical charged surface lies in their future application in electrical engineering for the development of capacitors with hemispherical geometry, which requires prior knowledge of the electric field created by these systems.

## MATERIALS AND METHODS

Analytical integration of Coulomb's law for the calculation of the electric field created by an homogeneously charged solid hemisphere of density  $\rho$  and volume  $V$  along its symmetry axes is presented in this article. The analytical integration of this vector field is developed by two different paths where the superposition principle is applied. On one hand, superposition of the electric field created by volumetric finite disks of increasing radius (see Figure 1) was performed. On the other hand, direct integration of finite elements of volume  $dV$  in cylindrical coordinates along the system volume was developed (Figure 2). The same result is obtained by the two ways. Classical integration techniques, which may be found in the bibliography (Pauly, 1909; Spivak, 1996), were used for this task.

Numerical integration based on superposition of  $N$  discrete randomly placed charges along the volume system ( $V$ ) was performed in order to validate the analytical solution. The computer program, developed with MATLAB, was executed in a CPU Intel Core i7-4700MQ with 2.40GHz and 20GB RAM memory. The time of integration for the case of  $N = 10^7$  discrete charges along  $n = 2001$  points over the symmetry axes was less than 292 seconds. Average deviation between analytical and numerical solutions for this case was less than 0.00005%, due to numerical error. Some numerical integration methods used with MATLAB can be found in the bibliography (Mathews & Fink, 1999; Notaros, 2014).

## RESULTS AND DISCUSSION

### 1. Analytical solution via disk superposition

Let us consider a solid hemisphere homogeneously charged with radius  $R$ . A calculation of electric field along its symmetry axes at a distance  $x_0$  from the center of the system (equatorial plane) is attempted.

The solution proposed in this paragraph is based on the superposition of homogeneous charged disks, with increasing radius  $r$  and finite thickness  $dx$ , as is shown in Figure 1. On the contrary, of hemisphere charged surface (del Vigo & Renedo, 2016), in this case, is not necessary to consider thickness disk length such a finite arc, because all the charge is homogeneous distributed along the entire disk volume of width  $dx$ . The approximation is obviously poorer for the disks that are near to the hemisphere pole, however, this effect is negligible, as will be discussed at the end of this paper. According to the bibliography, electric field of any disk at a distance  $d = x_0 - x$  is:

$$\vec{E}_{disk} = 2\pi k\sigma \cdot \left( \frac{d}{|d|} - \frac{d}{\sqrt{r^2 + d^2}} \right) \hat{i} \quad [1]$$

Where  $x_0$  is a fix point, while  $x$  varies along  $[-R, 0]$  depending on the position of the disk inside the hemisphere. This electric field is parallel to the symmetry axes (X-axis), what implies that electric hemisphere field will be too, due to the system symmetry. It might be notice that, the sign of equation [1] determines the positive/negative direction of the field; then, the absolute value over the distance is needed at the first term of this equation to ensure right direction for any value of  $X_0$ . The simplification of this equation is sometimes given in the literature as  $\frac{d}{|d|} = 1$ , for the study of a single disk in the origin system, restricted to the positive axes- $X^+$ .

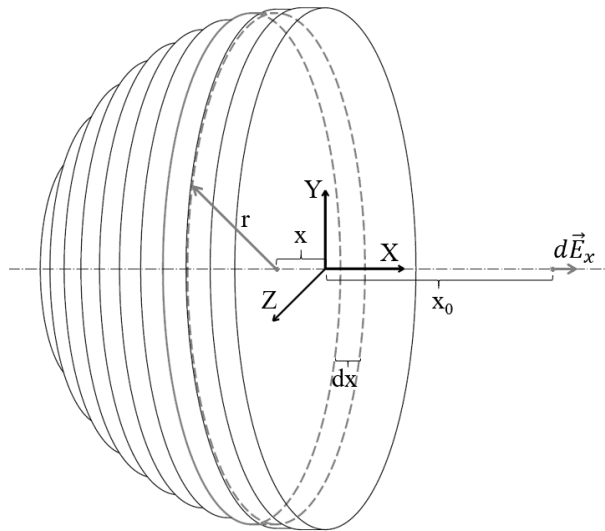


**Figure 1.** Hemisphere disk superposition. Electric field of each disk is known at a distance:  $d = x_0 + x$

Approximating to a finite thickness disk ( $dx$ ), the superficial density converts into a volumetric density of charge:

$$\sigma = \frac{Q}{\pi \cdot r^2} = \rho \cdot dx \quad [2]$$

Thus, the electric field for each finite element becomes to:

$$d\vec{E} = 2\pi k\rho \cdot \left( \frac{x_0 - x}{|x_0 - x|} - \frac{x_0 - x}{\sqrt{R^2 - x^2 + (x_0 - x)^2}} \right) \hat{i} \cdot dx \quad [3]$$

Where Pythagoras identity have been used in the last equation for the radius of each disk:  $r^2(x) = R^2 - x^2$ . Applying, superposition principle, electric hemisphere field is obtained by integration of equation [3]:

$$\vec{E} = \int_{-R}^0 d\vec{E} = 2\pi k\rho\hat{i} \cdot \int_{-R}^0 \left( \frac{x_0 - x}{|x_0 - x|} - \frac{x_0 - x}{\sqrt{R^2 + x_0^2 - 2x_0 \cdot x}} \right) dx \quad [4]$$

Where this integral is defined along the hemisphere limits. Since the unit vector  $\hat{i}$  is a constant, it can be extracted from the integral. From here, the problem becomes to the solution of integral [4]. For the sake of simplicity, let us rename the terms as:

$$I_1 = \frac{x_0 - x}{|x_0 - x|} = \begin{cases} 1; & x < x_0 \\ -1; & x > x_0 \end{cases} \quad [5.a]$$

$$I_2 = \frac{x_0 - x}{\sqrt{R^2 + x_0^2 - 2x_0 \cdot x}} \quad [5.b]$$

Integral of [5.a] is direct for each subdomain:

$$\int_{-R}^0 I_1 dx = \begin{cases} \int_{-R}^0 -dx = -R & x_0 < -R \\ \int_{-R}^{x_0} dx + \int_{x_0}^0 -dx = 2x_0 + R & -R < x_0 < 0 \\ \int_{-R}^0 dx = R & x_0 > 0 \end{cases} \quad [6]$$

and, integral of [5.b] is the sum of two simpler integrals:

$$\int_{-R}^0 I_2 dx = \int_{-R}^0 \frac{x_0}{\sqrt{R^2 + x_0^2 - 2x_0 \cdot x}} dx + \int_{-R}^0 \frac{-x}{\sqrt{R^2 + x_0^2 - 2x_0 \cdot x}} dx \quad [7]$$

where, the first one is direct:

$$\begin{aligned} \int_{-R}^0 \frac{x_0}{\sqrt{R^2 + x_0^2 - 2x_0 \cdot x}} dx &= |R + x_0| - \sqrt{R^2 + x_0^2} \\ &= \begin{cases} -(R + x_0) - \sqrt{R^2 + x_0^2} & x_0 < -R \\ (R + x_0) - \sqrt{R^2 + x_0^2} & x_0 > -R \end{cases} \end{aligned} \quad [8]$$

and, the second one, may be integrated by parts:

$$\left[ dv = \frac{dx}{\sqrt{R^2 + x_0^2 - 2x_0 \cdot x}} \Rightarrow v = -\frac{1}{x_0} \sqrt{R^2 + x_0^2 - 2x_0 \cdot x} \right] \Rightarrow$$

$$\Rightarrow \left[ x \cdot \frac{1}{x_0} \sqrt{R^2 + x_0^2 - 2x_0 \cdot x} \right]_{-R}^0 - \frac{1}{x_0} \int_{-R}^0 \sqrt{R^2 + x_0^2 - 2x_0 x} \cdot dx \quad [9]$$

Solving the last direct integral, substituting the integration limits and simplifying the absolute values, yields:

$$\frac{1}{3x_0^2} \left( (R^2 + x_0^2)^{\frac{3}{2}} + 3x_0 \cdot R \cdot |R + x_0| - |R + x_0|^3 \right) =$$

$$= \begin{cases} \frac{1}{3x_0^2} \left( (R^2 + x_0^2)^{\frac{3}{2}} + R^3 + x_0^3 \right) & x_0 < -R \\ \frac{1}{3x_0^2} \left( (R^2 + x_0^2)^{\frac{3}{2}} - R^3 - x_0^3 \right) & x_0 > -R \end{cases} \quad [10]$$

By reorganizing the results obtained in the equations [6]-[8]-[10], the electric field of a homogenous charged hemisphere, i.e., solution of equation [4] is:

$$\vec{E}(x) = \begin{cases} 2\pi k\rho \left[ x + \sqrt{R^2 + x^2} - \frac{1}{3x^2} \left( (R^2 + x^2)^{\frac{3}{2}} + R^3 + x^3 \right) \right] \hat{i} & x < -R \\ 2\pi k\rho \left[ x + \sqrt{R^2 + x^2} - \frac{1}{3x^2} \left( (R^2 + x^2)^{\frac{3}{2}} - R^3 - x^3 \right) \right] \hat{i} & -R \leq x \leq 0 \\ 2\pi k\rho \left[ -x + \sqrt{R^2 + x^2} - \frac{1}{3x^2} \left( (R^2 + x^2)^{\frac{3}{2}} - R^3 - x^3 \right) \right] \hat{i} & x > 0 \end{cases} \quad [11]$$

Where, correspondence  $x_0 \equiv x$  was used to remarks that this electric field is a function of the general Cartesian coordinate ( $x$ ).

## 2. Analytical solution via cylindrical coordinates

A direct integration of the electric field in cylindrical coordinates is presented in this paragraph. According to the body geometry, a finite volume element charge is:

$$dq = \rho \cdot dV = \rho \cdot dx dy dz = \rho \cdot r dx dr d\theta \quad [12]$$

Where the X-axis is taken, in this case, as the system symmetry axes and Jacobian of basis transformation is defined as  $|J| = r$  in last equation. Details of finite element volume ( $dV$ ) are given in the figure bellow. The approximation is valid because the finite elements are small enough to neglect curvature along its sides.

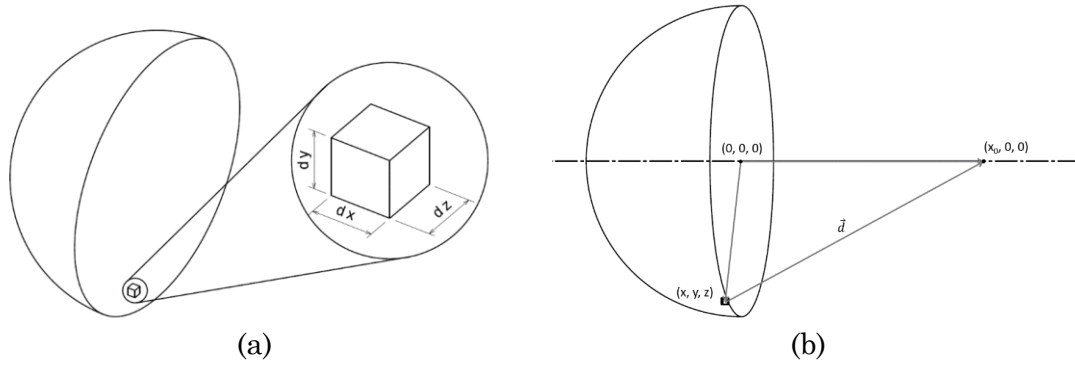


**Figure 2.** (a) Volume of each finite element. (b) Distance of any charge element to the point where electric field is calculated.

Coulomb's law is applied to each finite element on the hemisphere domain  $\aleph: (x, y, z)$ . A distance  $\vec{d}$  is defined between each finite element and the point of interest  $P = (x_0, 0, 0)$ , where the electric field is calculated. Transformation between Cartesian and cylindrical coordinates is used:

$$\begin{aligned} \vec{d} &= (x_0, 0, 0) - (x, y, z) = (x_0 - x, -y, -z) \\ &= (x_0 - x, -r \cos \theta, -r \sin \theta) \end{aligned} \quad [13.a]$$

$$d\vec{E} = k \cdot \frac{dq}{|d|^2} \cdot \hat{d} \quad [13.b]$$

It might be noticed that, the components of the equation [13.a] are defined in cylindrical coordinates, even though vector  $\vec{d}$  is still expanded on Cartesian basis:  $\mathcal{B} = \{\hat{i}, \hat{j}, \hat{k}\}$ ; in this way, the unit vectors may be extracted from the integrals. The combination of equations [12]-[13] yields an infinitesimal electric field for each charged element:

$$d\vec{E} = \frac{k\rho \cdot r dx dr d\theta}{((x_0 - x)^2 + r^2)^{\frac{3}{2}}} \cdot (x_0 - x, -r \cos \theta, -r \sin \theta) = (dE_x, dE_y, dE_z) \quad [14]$$

By applying the superposition principle for each element, a definite integral over the hemisphere domain,  $\aleph: (x, y, z)$ , emerges. Thus, an integral for each component must be solved.

First, y-component:

$$E_y = k\rho \cdot \int_{-R}^0 \int_0^{\sqrt{R^2 - x^2}} \frac{-r^2 \cdot dx dr}{((x_0 - x)^2 + r^2)^{\frac{3}{2}}} \int_0^{2\pi} \cos \theta d\theta = 0 \quad [15.a]$$

which is zero because the angular integral. Secondly, z-component:

$$E_z = k\rho \cdot \int_{-R}^0 \int_0^{\sqrt{R^2 - x^2}} \frac{-r^2 \cdot dx dr}{((x_0 - x)^2 + r^2)^{\frac{3}{2}}} \int_0^{2\pi} \sin \theta d\theta = 0 \quad [15.b]$$

that also is zero due to the angular integral. And finally, the x-component, what is not zero:

$$E_x = k\rho \cdot \int_{-R}^0 \int_0^{\sqrt{R^2-x^2}} \int_0^{2\pi} \frac{r \cdot (x_0 - x)}{((x_0 - x)^2 + r^2)^{3/2}} d\theta dr dx \quad [16]$$

$$= 2\pi k\rho \int_{-R}^0 (x_0 - x) \int_0^{\sqrt{R^2-x^2}} \frac{r}{((x_0 - x)^2 + r^2)^{3/2}} dr dx$$

This integral over radius is direct (considering  $x = cte$ ):

$$\left[ -((x_0 - x)^2 + r^2)^{-1/2} \right]_0^{\sqrt{R^2-x^2}} = \frac{1}{|x_0 - x|} - \frac{1}{\sqrt{(x_0 - x)^2 + |R^2 - x^2|}} \quad [17]$$

where  $|R^2 - x^2| = R^2 - x^2$ , because  $x \in (0, -R)$ . As a consequence:

$$\vec{E} = E_x \hat{i} = 2\pi k\rho \hat{i} \cdot \int_{-R}^0 \left( \frac{x_0 - x}{|x_0 - x|} - \frac{x_0 - x}{\sqrt{R^2 + x_0^2 - 2x_0 \cdot x}} \right) dx \quad [18]$$

The equation [18] is the same as equation [4] that was solved in the previous paragraph; thus, the same result is obtained for the electric field as a function of  $x \equiv x_0$  given at equation [11]:

$$\vec{E}(x) = \begin{cases} 2\pi k\rho \left[ x + \sqrt{R^2 + x^2} - \frac{1}{3x^2} \left( (R^2 + x^2)^{3/2} + R^3 + x^3 \right) \right] \hat{i} & x < -R \\ 2\pi k\rho \left[ x + \sqrt{R^2 + x^2} - \frac{1}{3x^2} \left( (R^2 + x^2)^{3/2} - R^3 - x^3 \right) \right] \hat{i} & -R \leq x \leq 0 \\ 2\pi k\rho \left[ -x + \sqrt{R^2 + x^2} - \frac{1}{3x^2} \left( (R^2 + x^2)^{3/2} - R^3 - x^3 \right) \right] \hat{i} & x > 0 \end{cases} \quad [11]$$

### 3. Discussion of the analytical solution

In this paragraph, the analytical solution obtained at [11] is analyzed to check its validity:

- (a) *Units*: [N/C] as expected.
- (b) *Continuity*: the solution is continuous within the three subdomains where is defined. Furthermore, continuity is guaranteed because the lateral limits on the boundaries of the subdomains coincide with the function values at these points:

$$\lim_{x \rightarrow -R^-} \vec{E}(x) = \lim_{x \rightarrow -R^+} \vec{E}(x) = -2\pi k\rho \cdot \frac{3 - \sqrt{2}}{3} R \cdot \hat{i} = \vec{E}(x = R) \quad [19.a]$$

$$\lim_{x \rightarrow 0^-} \vec{E}(x) = \lim_{x \rightarrow 0^+} \vec{E}(x) = \pi k\rho R \cdot \hat{i} = \vec{E}(x = 0) \quad [19.b]$$

Equation [19.b] was obtained after applying L'Hopital rule to solve a 0/0 indetermination. Thus, continuity of the solution is guaranteed.

- (c) *Electric field inside the body*: from the literature is known that the electric field inside a sphere grows linearly with radius (Burbano *et al*, 2004; del Vigo & Villarino, 2020). On the contrary, in this case, evolution with  $x$  coordinate is not a linear function inside the hemisphere. This behavior is caused by the lack of symmetry due

to the absence of the opposite hemisphere. Figure 3 represents the electric field intensity. It might be notice that, the electric field is not a straight line within the hemisphere; on the contrary, it is a convex curve.

- (d) *Discrete charge tendency for large distance*: analysis by Taylor series at [11] may prove that electric field tends to zero as a discrete charge ( $|E| \propto r^{-2}$ ) when  $x \gg R$ , in both directions.
- (e) *Symmetry*: electric field intensity is not symmetrical from X-axes. The small curvature shown in Figure 3b proves this fact; furthermore, it might be noticed that, the maximum-minimum values for equation [11] (at the hemisphere surface) does not coincides:

$$|E(x = -R)| = \left| \frac{2(\sqrt{2} - 3)}{3} \right| \pi k \rho R > \pi k \rho R = E(x = 0) \quad [20]$$

Remarks that, the electric field intensity is lower at the equatorial plane of the hemisphere ( $x = 0$ ) than at the pole ( $x = -R$ ), because the electric field produced by the charge that is around the equatorial plane is canceled at the point  $x = 0$ .

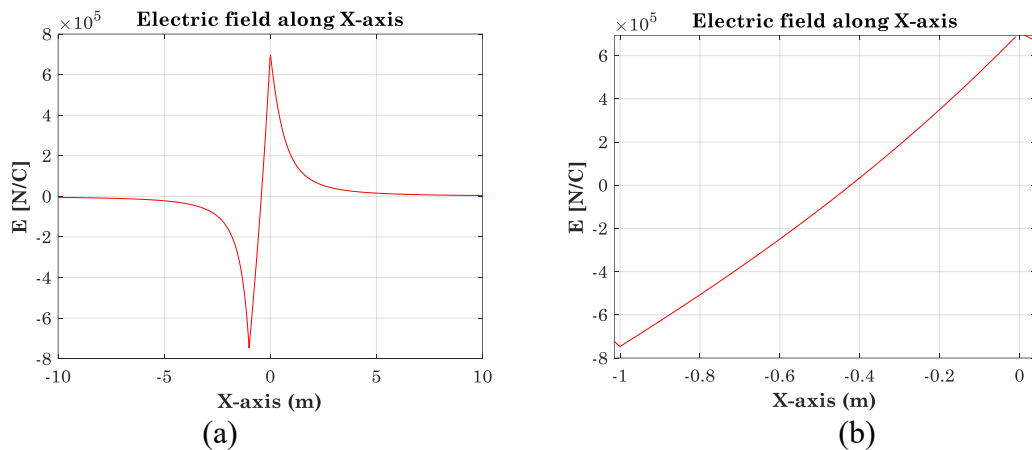


**Figure 3.** (a) Electric field intensity along X-axes of a homogenous charged hemisphere ( $Q = 0.1 \text{ mC}, R = 1 \text{ m}$ ). (a)  $x \in [-10, 10]$ , (b) Electric field intensity inside the body  $x \in [-1, 0]$ ; it is not a straight-line tendency since there exists a small convex curvature

#### 4. Numerical validation

A MATLAB routine was performed for comparison with the analytical solution. A fixed number of discrete charges ( $N$ ), were randomly placed along the volumetric charged hemisphere with radius  $R = 1 \text{ m}$ . A total charge  $Q = 0.1 \text{ mC}$  homogenously spread was introduced. The approximated hemisphere electric field was obtained by the sum of the electric field of each charge along the X-axis (superposition principle). The X-axis was defined as an array with  $n = 2001$  components. Figure 4 presents the numerical results obtained for  $N = 10^7$  discrete charges of  $q = 10^{-11} \text{ C}$  each (black line) in front of the analytical solution (red line). It might be noticed that, both curves apparently coincide. The average difference calculated between these two curves is around 0.4% (see Table 1). This small difference is assumed to be due to the error in the numerical approximation. Thus, validity of analytical proposed solution is confirmed. Although the numerical results are close to the analytical results, small differences occur due to the limitations of the

numerical approximation, especially in the electrode edge area (Romero-Mendez & Berjano, 2023).

A study of the convergence for numerical approximation is given at Table 1, based on the average of positives differences found between analytical ( $E_a$ ) and numerical ( $E_n$ ) electric field intensity along the symmetry axis. Relative uncertainty ( $E_{\%}$ ) is also presented in this table. Equation [21] express these error functions, where positive differences between numerical and analytical electric field intensity ( $E_n, E_a$ ) were calculated over the  $n = 2001$  points in the X-axis, within the interval  $x \in [-10,10]$ :

$$Error = \langle E_a - E_n \rangle = \sum_{i=1}^n \frac{|E_{a,i} - E_{n,i}|}{n} \tag{21.a}$$

$$E_{\%} = \left\langle \frac{E_a - E_n}{E_n} \right\rangle = \sum_{i=1}^n \frac{|E_{a,i} - E_{n,i}|}{|E_{n,i}|} \frac{1}{n} \times 100 \tag{21.b}$$

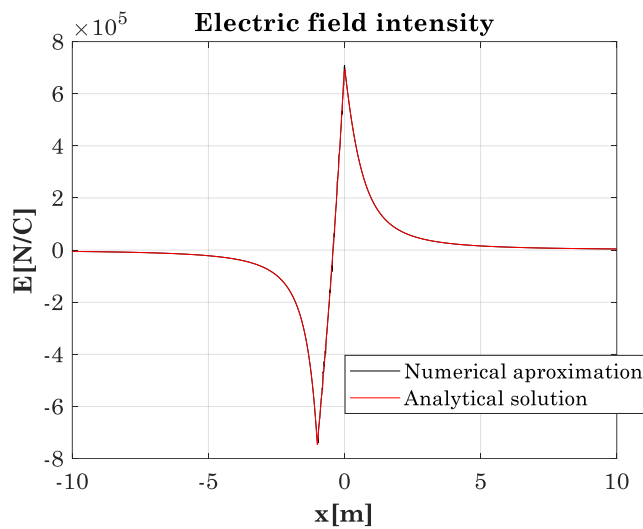


**Figure 4.** Analytical solution vs numerical approximation for  $N = 10^7$  discrete charges. Total hemisphere charge:  $Q = 0.1 \text{ mC}$ . Difference between numerical and analytical functions is around 0.4% in this case (see Table 1).

**Table 1.** Study of the numerical convergence to analytical solution.  $Error \propto \frac{1}{\sqrt[4]{N}}$ .

N	$10^3$	$10^4$	$10^5$	$10^6$	$10^7$	$10^8$
q (C)	$10^{-7}$	$10^{-8}$	$10^{-9}$	$10^{-10}$	$10^{-11}$	$10^{-12}$
Error (N/C)	9418	6155	3385	970	414	230
$E_{\%}$	4.775	3.046	1.429	1.009	0.414	0.094

Relative uncertainty function ( $E_{\%}$ ) represents the average difference, in percentage, between analytical and numerical solutions. It might be noticed that (Table 1), this statistical parameter decrease with the number of discrete charges ( $N$ ) used for the numerical approximation. In the case of  $N = 10^8$  discrete charges ( $q = 10^{-12} \text{ C}$ ) deviation between numerical approximation and analytical solution is lower than 0.1%. When using the Finite Element Method (FEM) and Boundary Method (BEM), a reduction in numerical uncertainty or error is often achieved by increasing the number of discrete elements in the

model. As the number of discrete elements increases, the difference between the numerical and analytical solutions decreases, confirming the validity of the analytical solution, which is also supported by related research on electric field optimization through a finer discretization approach in FEM and BEM to improve the accuracy of the numerical solution (Lee & Koh, 2018; Faiz & Ojaghahi, 2002).

Figure 5 represents the average deviation ( $E_{\%}$ ) in front of  $1/\sqrt[4]{N}$ . It might be noticed that a linear tendency between this two parameters is found. A linear fit (red line) is shown in the same picture. Table 2 presents the parameters involved for this linear approximation:

$$E_{\%} = \frac{26.20}{\sqrt[4]{N}} + 0.03$$

**Table 2.** Linear fit parameters for average deviation ( $E_{\%}$ ) in front of  $1/\sqrt[4]{N}$

$m$	$\Delta m$	$b$	$\Delta b$
26.205	1.841	0.026	0.396

The small value found for parameter  $b = 0.026 \pm 0.396$  suggest that deviation between analytical and numerical solutions ( $E_{\%}$ ) tends to zero when the number of discrete charges ( $N$ ) is infinity. It might be noticed that, parameter  $b$  can be null according to its error bound ( $\Delta b$ ).

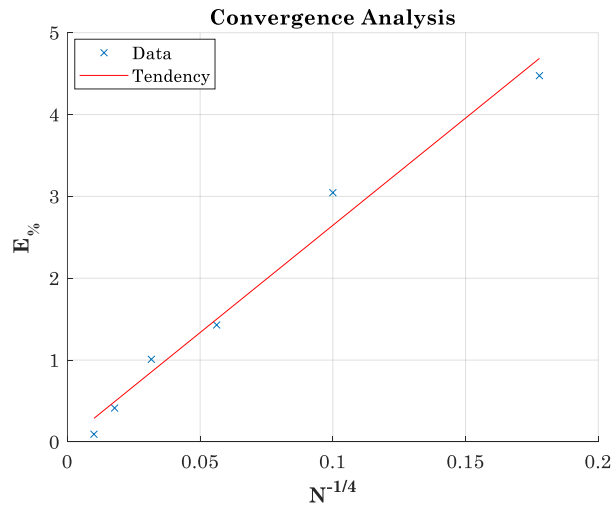


**Figure 5.** Convergence analysis,  $E_{\%} \cong \frac{25}{\sqrt[4]{N}}$ .

Some books of electromagnetism as Rodriguez (2002) have presented the solution of the electric field restricted at the center of the homogenously charged hemisphere. This theoretical result can be useful for the calculation of the capacity of two opposite hemispherical capacitor system throughout the classical methodology, that might be consulted in the bibliography (Tipler & Mosca, 2010; Servay & Vuille, 2018).

## CONCLUSIONS

The system symmetry let to calculate easily the electric field at this point when spherical coordinates are used for the integration. However, the solution for the entire symmetry axis that is proposed in this article is not found in the bibliography. The analytical solution proposed in this article was found by two different ways arising the same result. Furthermore, a numerical approximation to the analytical solution is given what definitely

confirms the solution obtained for the electric field of the hemisphere along its symmetry axis. Differences between analytical and numerical solutions becomes lower, and tends to zero, when increase the number of discrete charges that are used in the approximation ( $Error \propto 1/\sqrt{N}$ ). Then, the coincidence of these solutions can be assumed when  $N$  tends to infinity.

## ACKNOWLEDGMENTS

Authors want to thank Dr. Guadalupe Dorado for the English language review of this article.

## REFERENCES

- Burbano de Ercilla, S., Burbano, E. & García, C. (2004). *Problemas de Física General* (27<sup>o</sup> ed.). Tebar.
- del Vigo, Á. & Renedo, J. S. (2016). Campo eléctrico de una superficie semiesférica uniformemente cargada. *Revista 100cias-UNED*, 9, 185-190.
- del Vigo, Á. & Villarino, J. (2020). *Electricidad y Magnetismo. Problemas resueltos*. García Maroto Editores.
- Eisberg, R. M. & Lerner, L.S. (1988). *Física. Fundamentos y Aplicaciones*. Mc Graw-Hill.
- Faiz, J., & Ojaghi, M. (2002). Instructive Review of Computation of Electric Fields using Different Numerical Techniques. *Int. J. Engng Ed.*, 18(3), 344-356.
- Feynman, R. P., Leighton, R. & Sands, M. (1972). *Física (Vol.2): Electromagnetismo y Materia*. Addison-Wesley Iberoamericana.
- Griffiths, D. J. (2017). *Introduction to Electrodynamics* (4<sup>o</sup> ed.). Cambridge University Press.
- Jackson, J. D. (1998). *Classical Electrodynamics* (3<sup>o</sup> ed.). John Wiley & Sons.
- Lee, H & Koh, I. (2018). Consideration of diffraction effect in iterative physical optics combining physical theory of diffraction for conducting body. *12th European Conference on Antennas and Propagation (EuCAP 2018)*, London, UK, 2018, 1-5, <https://doi.org/10.1049/cp.2018.1186>.
- Mathews, J. H. & Fink, K. D. (1999). *Métodos Numéricos con MATLAB* (3<sup>o</sup> ed.). Prentice Hall
- Notaros, B. M. (2014). *MATLAB-Based Electromagnetics*. Pearson.
- Pauly, J. (1909). *Notions Élémentaires du Calcul Différentiel et du Calcul Intégral*. Librairie Polytechnique Ch. Béranger.
- Purcell, E. M. (1988). *Electricidad y Magnetismo* (2<sup>o</sup> ed.). Reverte.
- Rodríguez, V. L. (2002). *Electromagnetismo*. UNED.
- Romero-Mendez R, Berjano E. (2023). Differences in the Electric Field Distribution Predicted with a Mathematical Model of Cylindrical Electrodes of Finite Length vs. Infinite Length: A Comparison Based on Analytical Solution. *Mathematics*, 11(21), 4447. <https://doi.org/10.3390/math11214447>.
- Serway, R. A. & Vuille. C. (2018). *College Physics* (11<sup>o</sup> ed). Cengage.
- Spivak, M. (1996). *Calculus* (2<sup>o</sup> ed.). Reverte.
- Tipler, P.A. & Mosca, G. (2010). *Física para la ciencia y tecnología* (6<sup>o</sup> ed.). Reverte.